

The Effect of Honing Speed and Grain Size on Surface Roughness and Material Removal Rate during Honing

Damir Vrac¹, Leposava Sidjanin², Sebastian Balos²

¹IMR-Rakovica, Patrijarha Dimitrija 7-13, 11000 Belgrade, Serbia
office@imr.co.rs

²Department of Production Engineering, Faculty of Technical Sciences,
University of Novi Sad, Trg Dositeja Obradovica 6, 21000 Novi Sad, Serbia
lepas@uns.ac.rs, sebab@uns.ac.rs

Abstract: In this paper, an attempt was made to study the dependencies between average and maximum roughness in relation to material removal rate and specific volume material removal rate of long-stroke honing in relation to different abrasive grain size tools and honing speeds. Long-stroke honing was performed on grey cast iron cylinder liners. It was found that by using a finer grain tool, lower roughness and similar material removal rate is obtained. Inconsistent relation between average and maximum roughness in relation to material removal rate and specific volume material removal rate were described by abrasive grain stress in honing tools. Abrasive grain stress influences the fall-out of abrasive grains from the tool surface and their uncontrolled movement over the sample – tool system. This results in a stochastic workpiece material removal, which is more severe if the abrasive grains are larger in the corresponding tool.

Keywords: long-stroke honing; honing speed; abrasive grain stress

1 Introduction

Automotive industry components, such as cylinder sleeves, crankpins and camshaft lobes, valve seat and valve guides, valve body, high pressure pump components, etc. need lubrication, which demands a unique surface texture. This is achieved by plateau honing, obtained in two machining operations: pre – honing or rough honing with large abrasive grain size and subsequent finishing or fine honing with small abrasive grain size [1], [2]. Rough honing induces deep creases of specific geometry for effective lubricant retention [3], [4]. The smooth surface between the deep creases are machined to reduce wear and enable sealing - finishing honing [5], [6]. A typical surface profile obtained by plateau honing is shown in Figure 1 [7].



Figure 1

Surface texture profile showing: a) pre-honing profile and b) obtaining final profile by finishing honing [7]

An even higher quality of surface topography compared to plateau honing is obtained by the application of long-stroke honing [8]. In long-stroke honing, certain surface texture features, such as surface marbling, sheet metal cover build up and plastic deformation are not allowed [9]. Furthermore, creases are narrower, reducing the amount of lubricant in the cylinder inner surface. This results with a lower oil consumption and therefore a lower pollution [10]. Finally, In [9] – [11] it was found that the absence of sheet metal cover reduces engines running in times, as well as that sheet metal cover may reduce the flow or even prevent oil flow.

Long-stroke honing is achieved by applying lower kinematic parameters compared to plateau honing, resulting in lower material removal rate [12]. Robota and Zwein [13] discussed the application of laser structural honing and electrochemical honing for pre-honing, while mechanical honing process is used for finishing honing. A similar technique was thoroughly explained by Degner and Borcal [14], [15], Guo-Qiang [16] and modelled by Shaikh [17]. However, in [18] – [20], the possibility for application of mechanical pre-honing instead of electrochemical honing was found to be feasible. The application of mechanical honing for both pre- and finishing honing can make the whole honing machining process simpler and more flexible. On the other hand, a careful optimization is required, in the terms of application of adequate honing stones, as well as process parameters to achieve the required roughness and material removal rate.

In previous papers by Vrac *et al.*, dispersion analysis was conducted to develop mathematical models for pre-honing parameter influence on surface roughness and material removal rate parameters [18] – [20]. Mathematical models were developed to determine the most influential pre-honing parameters. It was found that the most influential parameter on average roughness is specific honing pressure, over feed and honing speed [18]. On the other hand, in [19], when coarser grained tool was used, honing speed had a higher impact on maximum roughness than specific honing pressure. However, specific honing pressure was more significant than honing speed when a finer grained tool was applied [19].

Similarly, in [20] honing speed was found to be more influential on maximum peak height than feed and depth of cut, when coarser grained tool was used. When a finer abrasive grain tool was used, the parameter with the highest impact on maximum peak height was feed, followed by honing speed and depth of cut. The most influential parameter on material removal rate was honing speed, followed by specific honing pressure, feed and depth of cut [20].

In this paper, an attempt was made to obtain a graphical interpretation of the influence of honing speed and abrasive grain size on material removal rate, specific volume material removal rate, maximum and average roughness, in order to maximise advantages, such as surface texture – roughness parameters and minimise the main drawback of long-stroke honing, low material removal rate.

2 Experimental Study

In this study, experimental investigation was done on dry cylinder liners used on IMR DM-33 tractor diesel engine. Workpiece material used in this study was GJL 250 grey cast iron, in accordance to [21]. Chemical composition, tested by Beckman DU-2 optical emission spectrometer is given in Table 1. Microstructure was analyzed after standard metallographic preparation technique and etching with Nital, by Leitz Orthoplan light microscope (LM), Figure 2. From Figure 2a, it can be seen that flake graphite belongs to B-type with traces of C-type graphite, and with IB4 distribution [22]. Metal matrix microstructure consists of pearlite, a small amount of ferrite and phosphide eutectic, Figure 2b,c. The size of phosphide eutectic eyes is uniform, forming dense and closed network, Figure 2c. Brinell hardness was tested by Wolpert DIA Testor Z testing machine, while ultimate tensile strength was determined by Amsler 40 SZBDA 699 machine. Hardness of the grey cast iron was 250 ± 5 BHN, while ultimate tensile strength was 280 ± 10 MPa.

Table 1
Chemical composition of GJL-250 grey cast iron [mass %]

C	Si	Mn	P	S	Cr	Fe
2.80	2.21	0.61	0.02	0.02	0.35	balance

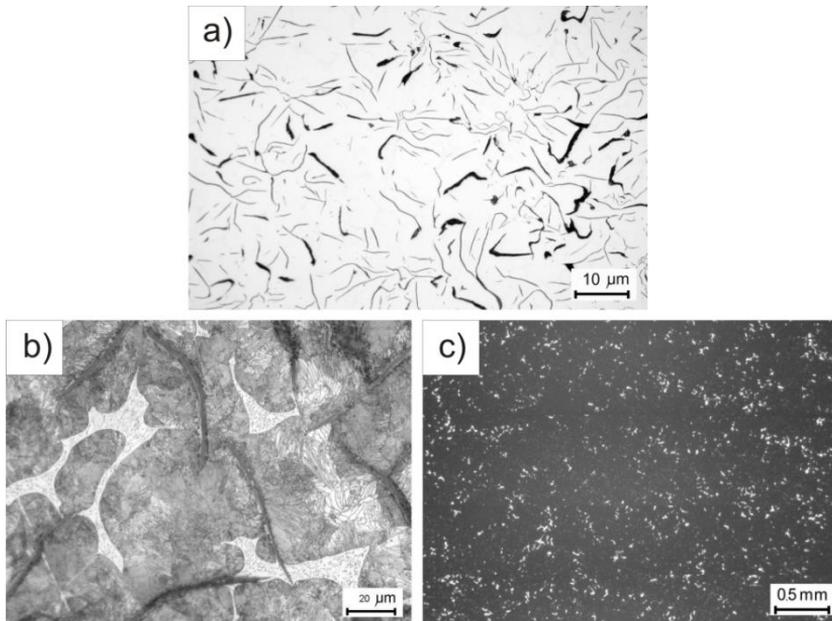


Figure 2

Workpiece material – graphite shape (a), metal matrix microstructure - pearlite + ferrite isles (b) and phosphide eutectic network (c)

Input parameters, tool specifications and work piece dimensions were as follows:

Input parameters:

Circumferential speed	$v_k=51.70; 57.488; 63.193$ m/min
Axial speed	$v_a=21.205; 23.477; 27.263$ m/min
Pressure	pre-honing $p=10; 12; 14$ bar; finishing honing: 2, 3, 4 bar
Crossing angle	$\alpha=36-55^\circ$ (D151 tool); $34-54^\circ$ (D181 tool)
Coolants and lubricants	Honol-2 (kinematic viscosity $10-12$ mm ² /s), $Q=10$ l/min (pre-honing); 14 l/min (finishing honing)
Allowance	$z=0.025-0.030$ mm
Length of stroke	$L=189.33$ mm
Number of double strokes:	$n_k=52-72$ min ⁻¹

Tool specification:

Pre- and finishing honing head: HLD-Nagel with six honing stones
Honing stones [23, 24]:

- pre-honing: 1. 5x5x80/2 mm /D 181/44/502M113/C50 Tyrolit 80/100 mesh
 (180 μm diamond grain size with bakelite bonding [20, 21])
 2. 5x5x80/2 mm/D 151/44/502M113/C75 Tyrolit 100/120 mesh
 (150 μm diamond grain size with bakelite bonding)
- finishing honing: 10x10x80 mm/ NK 280 Gu 4101 F5 Nagel 325/400 mesh (46
 μm SiC grain size with rubber bonding)

Work piece dimensions:

Diameter $D=94.478^{+0.025}$ (mm)

Length $L=216^{-0.2}$ (mm)

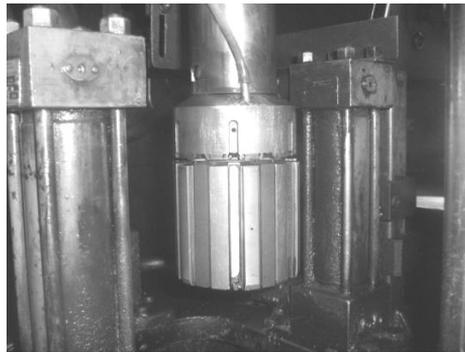


Figure 3

Honing tool with finishing honing stones

Pre-honing, which was the main subject of this work, was performed by applying three tool honing speeds: 0.93; 1.02; 1.11 m/s. Tool grain size and honing speeds were correlated to surface structure parameters and material removal rate parameters. Surface structure parameters (R_{max} ; R_a) were obtained with Rank Taylor Hobson Talysurf 6 profilometer, by using PMMA stamps. Material removal rate parameters, such as material removal rate (Q) and specific volume material removal rate (z) were found analytically. Honing material removal rate may be defined as the volume of the material cut in a second. Material removal rate may be expressed as:

$$Q_w = A_a v_a + A_t v_t + A_n v_n \quad (1)$$

where A_a , A_t , A_n are active contact areas between the tool and the work piece, v_a , v_t , v_n axial, tangential and normal honing speed components. Specific volume material removal rate [$\text{mm}^3/\text{mm}^2\text{s}$] may be expressed as:

$$Q'_w = \frac{\Delta V_w}{t \cdot A_H} \quad (2)$$

where: ΔV_w is material volume removed [mm^3], t honing time [s] and A_H – honing stone working surface [mm^2].

Honing speed was determined as the sum of vectors of v_k and v_a :

$$v_s = \sqrt{v_k^2 + v_a^2} \quad (3)$$

where v_s is honing speed [m/s], v_k is circumferential speed and v_a is axial speed.

After honing, samples were cut and coated with gold. Their surface textures were examined by scanning electron microscope (SEM) JEOL JSM 6460 LV, operating at 25 kV. Coating was done by using Balltec SCD-005 coating device. Honing stone surface before and after honing was observed by stereo microscope Leica M205A.

3 Results

3.1 Roughness Parameters - Material Removal Rate Dependences

Roughness parameters – material removal rate dependences are shown in Figs. 4-7. Values obtained in experimental investigation are shown in the form of square markers, while the values that correspond to the same honing speed applied were grouped in triangular or longitudinal form. Larger triangle or line segment indicate a larger deviation between the obtained results. Centroids of each triangle or line segment define trend lines that describe the relation between each specific roughness and material removal rate parameter. An ideal case is a horizontal line, which corresponds to the case where increasing material removal rate does not influence the increase in roughness.

Regardless of roughness parameter (R_a and R_{max}) – material removal rate parameter (Q and z) presented in Figs 4-7, very similar relations and trends were noticed. Triangle areas that refer to average roughness (R_a) – material removal rate (Q) dependence are larger when D181 tool was applied than those obtained with finer grained D151 tool, Figure 4. Exactly the same trend was noticed for other dependencies: maximum roughness (R_{max}) – material removal rate (Q), Figure 5; average roughness (R_a) – specific volume material removal rate (z), Figure 6 and maximum roughness (R_{max}) – specific volume material removal rate (z), Figure 7.

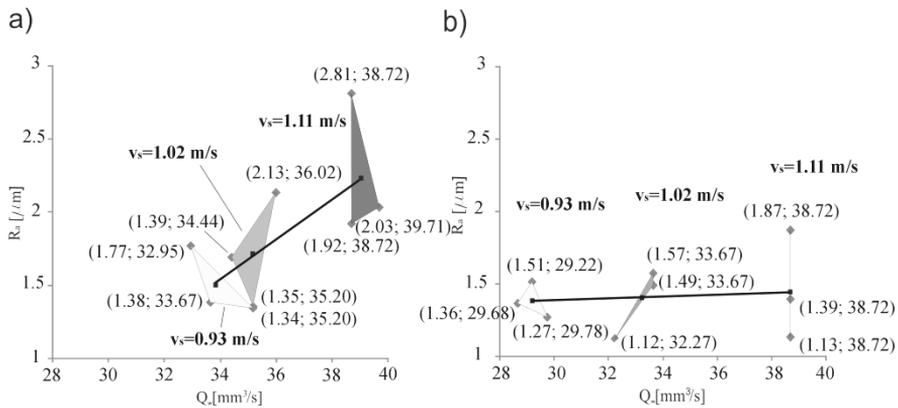


Figure 4

The dependence between average roughness R_a and material removal rate Q by using D181 (a) and D151 tool (b)

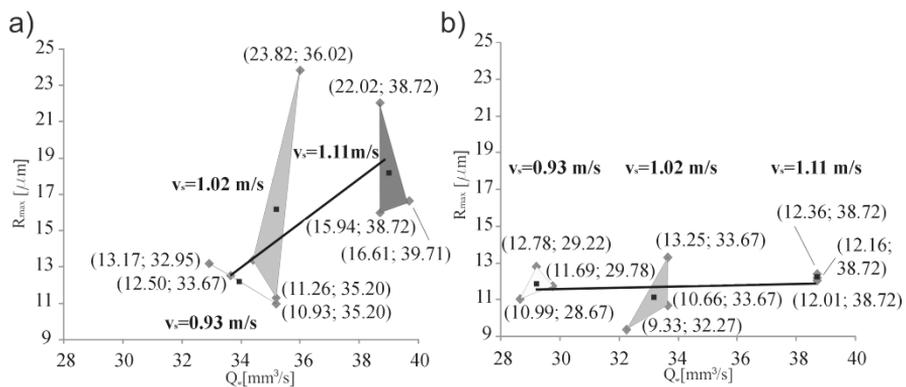


Figure 5

The dependence between maximum roughness R_{max} and material removal rate Q by using D181 (a) and D151 tool (b)

A considerable difference between D181 and D151 tool was noticed in trend lines obtained from centroids as well. Trend lines that describe roughness – material removal rate dependence obtained with D181 tool are more inclined compared to corresponding trend lines obtained with D151 tool, Figs. 4-7. It should be noted, that the trendlines obtained from the centroids of experiments conducted with D151 tool are nearly horizontal, which is close to the ideal, horizontal trend that indicates no change in roughness parameter at higher material removal rate parameter.

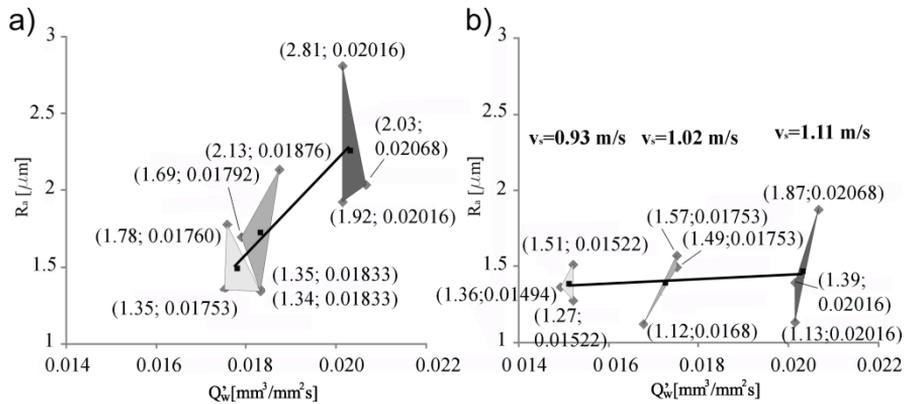


Figure 6

The dependence between average roughness R_a and specific volume material removal rate z by using D181 (a) and D151 tool (b)

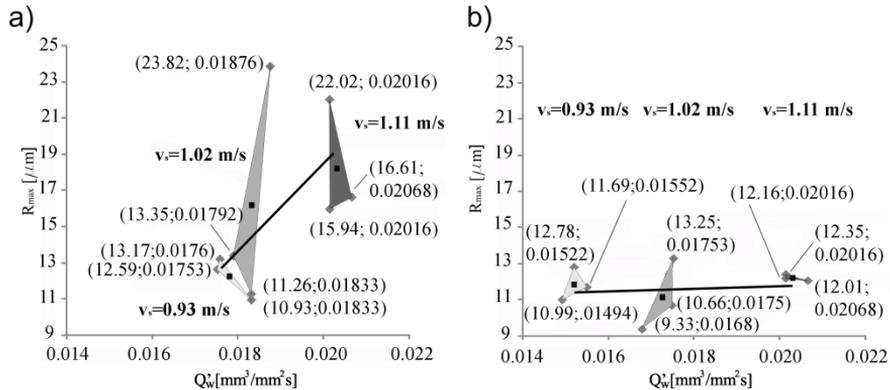


Figure 7

The dependence between maximum roughness R_{max} and specific volume material removal rate z by using D181 (a) and D151 tool (b)

3.2 Workpiece and Honing Stone Surface Textures

Surface texture after honing obtained with D181 tool, as well as crossing angle α is shown in Figure 8. As can be seen, no marbling, sheet metal cover build up and plastic deformation is present. Deep creases can be observed, suitable for lubricant flow along the path of the cylinder. These creases are straight, indicating that they are produced by a combined – axial and radial tool movement. However, one curved crease shown by a white arrow can be observed, which was clearly obtained differently.

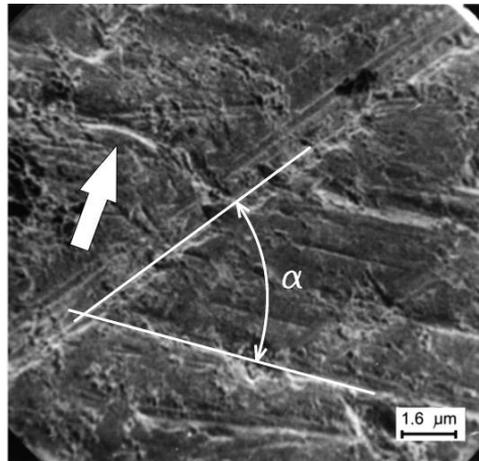


Figure 8

Surface texture obtained with D181 tool, where white arrow shows damage that may be caused by a fallen out diamond abrasive grain or grain fragment (SEM)

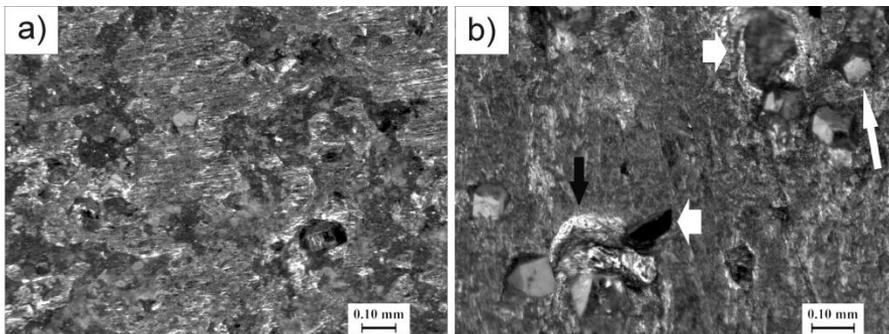


Figure 9

D151 honing stone surface: a) A relatively smooth surface with a small number of abrasive grains can be observed in an unused tool; b) An used D151 honing stone surface. Long white arrow shows the exposed abrasive grain, short white arrows show abrasive grain pits and black arrow points at a surface damage that may be the result of a fallen out abrasive grain

Surface texture of D151 honing stones before and after pre - honing process is shown in Figure 9. In Figure 9a, an undamaged surface can be observed, with a small number of exposed abrasive grains. On the other hand, in Figure 9b, a number of exposed abrasive grains are visible. Furthermore, some abrasive grains appear exposed (long white arrow), while some empty pits are visible (short white arrow).

4 Discussion

Trends shown in Figs. 4-7, related to triangle and line segment size are the result of larger differences between the obtained results within the same honing speed. These differences are predominantly related to roughness parameters. The highest differences within the same honing speed were noticed at maximum roughness by using a coarser grained D181 tool, Figs. 5 and 7, where this difference amounts up to 118 %. On the other hand, differences between maximum roughnesses by using a finer grained D151 tool were smaller, however, even in this case, the maximum difference reached 42%. If average roughness is considered, for both D181 and D151 tools, maximum differences are closer to maximum roughness differences obtained with D151 tool. In general, the values of R_a and R_{max} are comparable to the values obtained by Stout and Davies [25] as well as Stout and Spedding [26].

Material removal rate parameters shown in Figures 4-7 do not show a similar differences within the same honing speed as roughness parameters - maximum differences are within 10%.

Previous discussion indicates that by applying D181 tool, both material removal rate and specific volume material removal rate may be increased, but at the expense of increased roughness. However, by using D151 tool, trend line is almost horizontal, which means that an increased material removal rate and specific volume material removal rate can be obtained without a significant impact on average and maximum roughness. That means, material removal rate and specific volume material removal rate of the surface machined by a finer grain tool (D151) may have equal roughness parameters as with coarser grained tool (D181), but providing 15-20% higher material removal rate and specific volume material removal rate, Figures 4-7.

Although angle between trend lines and horizontal axis does indicate roughness – material removal rate dependence, which gives valuable informations about one of the most significant advantages of long-stroke honing and its most notable drawback, material removal rate, a special attention must be payed to relatively high differences between roughness parameters, most importantly maximum roughness, as key parameters of the surface texture obtained by long-stroke honing. When honing speed influence on roughness dispersion is considered, different results are obtained regarding maximum and average roughness. Maximum roughness differences within one experimental setup reach a maximum at medium honing speed at 1.02 m/s, after that, differences drop considerably. This drop is much more significant when a finer grained D151 tool is used. Average roughness obtained with both R181 and R151 tools rises with the increase in honing speed. One possible explanation of these phenomenons is tool-removed material interaction during honing. Namely, at higher honing speeds, the removed material aids in abrasive grain retention in the tool, promoting a decrease in maximum roughness. However, at higher honing speeds, more heat is produced in the bonding material, leading to a higher abrasive grain stress, where abrasive

grains can fall out from the tool. Fragments produced this way may influence an increased average roughness due to the induction of additional creases in the workpiece material, which can have an unpredictable shape, direction and profile, having an adverse effect on the lubricant flow. Clearly, a fallen – out grain would not follow the kinematic path of the grains still placed into the tool, but they would rather follow an unregular path, not necessarily straight. A crease shown by white arrow in Figure 8 is a representative example. The unregular grain or grain fragment movement in the workpiece – tool system is supported by the observations in the honing stone surface, Figure 9. A black arrow points at an unregular abrasive grain path in the tool surface, that can be the result of the abrasive grain fall out from the bakelite matrix. The appearance of the curved path in Figure 9b is similar to that shown in Figure 8 that refers to the workpiece surface. This supports the theoretical explanation of obtaining an increased roughness and irregular creases by applying high-end honing speeds tested in this study. The stochastic component is more pronounced if honing speeds are higher, as well as if the abrasive grains are larger.

Conclusion

In accordance to experimental analysis of GJL250 grey cast iron has shown that:

- Centroid derived trendlines indicate a stronger influence of honing speed on roughness-material removal rate dependence for a coarser-grained than a finer-grained pre-honing tool. This means a finer surface texture for the same material removal rate is obtained with a finer abrasive grain tool. On the other hand, for the same roughness parameters (average and maximum roughness), a higher productivity and specific volume material removal rate can be obtained. This increase in material removal rate is between 15 and 20%.
- Average and maximum pre-honing roughness results show a more significant differences within one experiment with a constant honing speed for a coarser-grained than a finer-grained pre-honing tool. Inconsistencies in peak differences between the results obtained at the same honing speed may be explained by abrasive grain stress.
- Abrasive grain stress may influence the falling out of abrasive grains from the honing stone. These grains have unpredictable trajectories over the workpiece surface, making irregular creases. As these creases are more pronounced, their impact on inconsistent lubricant flow is higher.

Finer grained tool and higher honing speed are beneficial for achieving higher material removal rate at a moderate rise of roughness parameters.

References

- [1] P. Stark: Feinbearbeitung in der Automobilindustrie, In Jahrbuch Schleifen, Honen, Läppen und Polieren, Vulkan-Verlag, Essen, Germany, 1985, pp. 458-496
- [2] MC. Malburg, J. Raja, DJ. Whitehouse, Characterization of Surface Texture Generated by Plateau Honing Process, CIRP Annals - Manufacturing Technology, 42 (1993) pp. 637-639
- [3] YB. Guo, Y. Zhang, JA. Zhong J. A. and K. Syoji: Optimization of Honing Wheel Structure Parameters in Ultra-Precision Plane Honing, Journal of Materials Processing Technology, 129 (2002) pp. 96-100
- [4] IB. Corral, JV. Calvet and MC. Salcedo: Use of Roughness Probability Parameters to Quantify the Material Removed in Plateau-Honing, International Journal of Machine Tools & Manufacture, 50 (2010) pp. 621-629
- [5] D. Vrac, L. Sidjanin and D. Milikic: The Influence of Honing Regime on Quality of Surface Finished by Honing, Proceedings of XXXII Conference on production engineering with foreign participants, Novi Sad, Serbia (2008) pp. 117-120
- [6] P. Pawlus, T. Cieslak and T. Mathia: The Study of Cylinder Liner Plateau Honing Process, Journal of Materials Processing Technology, 209 (2009) pp. 6078-6086
- [7] D. Vrac: Final Machining Process of Cylinder Liner of Internal-Combustion Engine, PhD thesis, Faculty of Technical Sciences, Department for Production Engineering, University of Novi Sad, Serbia, 2007
- [8] DIN 8589 Standard: Manufacturing processes chip removal – Part 0: General; Classification, subdivision, terms and definitions, Berlin, Germany (2003)
- [9] E. Sech and J. Strobel: Diamant fluidstrahl gätthnung. Friedrich Vieweg & Sohn Verlagsgesellschaft, 2001
- [10] D. Vrac: The Characterization of Honing Surface Roughness by Surface Reaction RSM Method, Proceedings of 9th international scientific conference MMA 2006 - Flexible technologies, Faculty of Novi Sad, Serbia: (2006) pp. 35-36
- [11] JK. Tyagi and VC. Krishnamurthy: On Surface Quality of Honed Surfaces, Proceedings of the 5th International Conference on Production Engineering, Tokyo, Japan (1984) pp. 708-713
- [12] D. Vrac: The Influence of Cylinder Machining on Techno-Exploitation Properties of a Typical Diesel Engine, M. S. Thesis. Faculty of Technical

- Sciences, Department for Production Engineering, University of Novi Sad, Serbia, 2003
- [13] A. Robota and F. Zwein: Einfluss der zylinderlaufflächentopografie auf den Ölverbrauch und die partikelemissionen eines DI-Dieselmotors. Friedrich Vieweg & Sohn Verlagsgesellschaft, 1999
- [14] J. Borcal: Unconventional Machining Processes, Czech high technical school 1989
- [15] W. Degner: Electrochemical Machining, VEB Verlag Technik, Berlin (1984)
- [16] W. Guo-Qiang, W. Zhao-Bing, C. Chi-Ping, Field-controlled Electrochemical Honing of Gears, Precision Engineering, 9 (1987) pp. 218-221
- [17] JH. Shaikh, NK. Jain: Modeling of Material Removal Rate and Surface Roughness in Finishing of Bevel Gears by Electrochemical Honing Process, Journal of Materials Processing Technology, 214 (2014) pp. 200-209
- [18] D. Vrac, L. Sidjanin and S. Balos: Mechanical Finishing Honing: Honing Regimes and Surface Texture, Industrial Lubrication and Tribology, 63 (2011) pp. 427-435
- [19] D. Vrac, L. Sidjanin, P. Kovac and S. Balos: The Influence of Honing Process Parameters on Surface Quality, Productivity, Honing Angle and Coefficients of Friction", Industrial Lubrication and Tribology, 64 (2012) pp. 77-83
- [20] D. Vrac, L. Sidjanin, S. Balos and P. Kovac: The Influence of Tool Kinematics on Surface Texture, Productivity, Power and Torque of Normal Honing, Industrial Lubrication and Tribology, 66 (2014) pp. 215-222
- [21] DIN EN 1561 Standard: Founding - Grey cast iron, Berlin, Germany (1997)
- [22] Adam Opel 107 Standard: Aktiengesellschaft Wekrstoff – Entwicklung, Rüsselsheim, Germany (1979)
- [23] DIN 69186 Standard: Honing stones, Berlin, Germany (1983)
- [24] ASTM E-11-2009 Standard: Standard Specifications for Wire Cloth and Sieves for Testing Purposes, West Conshohocken, USA (2009)
- [25] KJ. Stout and EJ. Davis: Surface topography of cylinder bores-the relationship between manufacture, characterization and function, Wear, 95 (1984) pp. 111-125
- [26] KJ. Stout and TA. Spedding: The Characterization of Internal Combustion Engine Bores, Wear, 83 (1982) pp. 311-326